Chapter 2

Characterization of Single Polymer Molecules

Milad Radiom

Additional information is available at the end of the chapter

http://dx.doi.org/10.5772/intechopen.77999

Abstract

This chapter offers an overview of the use of atomic force microscopy (AFM) in polymer studies. Soft AFM cantilevers with sharp tips are useful for their relatively high spatial resolution, a few nm, and force resolution, a few tens of pN. AFM imaging is used to characterize conformational properties of single polymer chains at solid-liquid interfaces. AFM force microscopy gives molecular elasticity as well as interaction forces of single polymer chains with solids. Recent technical developments have made possible the characterization of time-resolved mechanical properties of single polymer chains, including the relaxation time and internal friction. AFM force microscopy with biomolecules, supramolecules, and mechanophores reveals the forces required for, and the kinetics of, conformational transitions and chemical reactions in these molecules at the single-chain and single bond levels.

Keywords: AFM imaging, atomic force microscopy, mechanochemistry, molecular conformations, molecular elastic response, single molecule force microscopy, single molecules

1. Introduction

From the time of its invention in 1986 [1], atomic force microscopy (AFM) has been influential in polymer studies mainly at the nanoscale. The imaging mode of AFM has been used to visualize polymer chains [2, 3], while the force microscopy mode to measure their elasticity, internal friction, and adhesion forces [4–7]. Moreover, the long-established theories of polymer mechanics and dynamics could be reevaluated and retuned to better interpret the new results obtained from AFM measurements [8, 9]. Alongside theories, computational chemistry methods have been adopted to evaluate relevant experimental parameters from *ab initio* or molecular dynamics calculations, or to model the force response of polymers with conformational transition, for example polysaccharides [10, 11].

In imaging application, polymer chains are generally adsorbed from a dilute solution. The dilute condition results in thin polymer films where the chains are isolated. The polymers are deposited on flat solids such as mica, silica (due to roughness, silica is used with thick polymers such as dendronized polymers), gold (for example, gold deposited on mica), or highly oriented pyrolytic graphite (HOPG). The individual chains are then imaged using noncontact or intermittent contact imaging modes [12–17]. Analysis of AFM images provides useful information on conformations and sizes of polymer molecules, and conformational transitions because of changing chemical environment [3, 18–21]. Examples of AFM images of double-stranded DNA [3] and four generations of a dendronized polymer [22] are shown in **Figure 1 (a)** and **(b)**. Analysis of DNA images shows the effect of chemical environment, solution as well as solid substrate, on DNA conformation and length. Processing of the AFM images of dendronized polymers show that chains thicken with generation of dendronization, while their conformations persist over longer distances.

In a seminal work, Gaub and coworkers showed that AFM can be used to manipulate proteins at single molecule level [4]. This research led to the use of AFM in polymer studies involving the extension and manipulation of single polymer chains. The measurements are realized by adsorbing a polymer film on solid from a dilute to moderately concentrated polymer solution. The tip of the AFM cantilever is then brought into contact with the solid and retracted. This process results in occasional extension of a single chain. The solid substrate and the AFM tip can be functionalized to chemically bind the polymer chains, or to tune between extension and desorption interactions [5, 6]. To model the force versus extension profiles, the polymer chain is modeled with a continuous curve, or as a series of discrete segments that are freely jointed or jointed at fixed bond angles with rotational freedom [26]. These models normally incorporate a characteristic length corresponding to entropic elasticity of the polymer and a characteristic elasticity constant corresponding to deformation of bond angles. Examples of AFM force microscopy of poly(ethylene glycol) (**PEG**) [23] and single-stranded DNA [11] are shown in **Figure 1(c)** and **(d)**. In both cases, one observes that the force increases monotonically with extension. This is because the polymer chain loses its entropy during elongation causing a restoring force on AFM cantilever. Unlike the response of single-stranded DNA, **PEG** force response shows conformational transition in electrolyte solution. The transition is absent in non-hydrogen bonding hexadecane.

Among other developments, AFM single molecule force microscopy was combined with electrochemistry to obtain sequential extension-oxidation-relaxation giving a thermodynamic cycle with a single chain of a redox polymer [27]. Using two AFMs in parallel configuration, a correlation force microscope (CFM, or correlation force spectroscopy, CFS) was developed and used to measure the dynamics of single polymer chains, namely elasticity and relaxation time [7, 28]. Furthermore, by laterally dragging single polymer chains that are covalently bound to AFM tip and adsorbed onto solid, nanoscale friction mechanisms were investigated using a single polymer chain probe [29, 30].

AFM is also used to activate chemical reactions and conformational transitions at single polymer chain level. In this case, the polymers contain force-sensitive units, which are activated by application of mechanical force. Moreover, to measure the strength of chemical bonds, one may

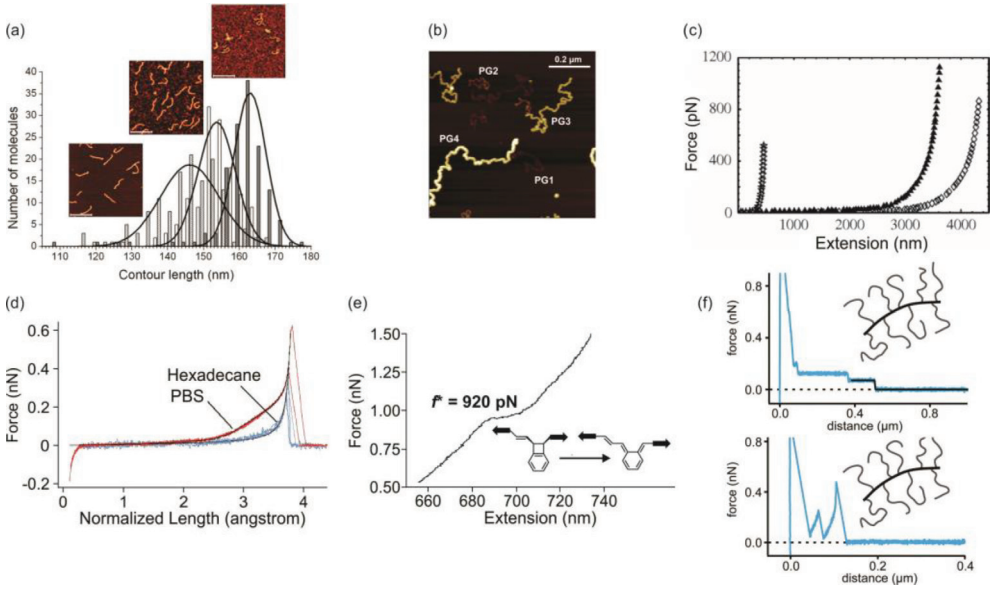

Figure 1. (a) AFM images of 500 base-pair DNA with the corresponding histograms of contour lengths. DNA deposited on (3-aminopropyl)triethoxysilane modified mica resulted in the longest length, while when deposited on mica from a solution containing Mg^{2+}, it resulted in the shortest length. Middle range length was for when DNA was deposited on mica from a solution containing Mn^{2+}. Adapted with permission from Japaridze et al. [3]. Copyright © 2016 American Chemical Society. (b) AFM image of generation 1–4 of a dendronized polymer that has two terminal amines per monomer adsorbed on mica. The image shows thickening and longer conformational persistence of the polymers with generation. Adapted with permission from Zhang et al. [22]. Copyright © 2011 American Chemical Society. (c) Force versus extension response of single-stranded DNA chains. The DNA was adsorbed on a gold-coated surface and extended in Tris buffer. Reprinted figure with permission from Hugel et al. [11]. Copyright (2005) by the American Physical Society. (d) Force versus extension response of poly(ethylene glycol) (**PEG**) polymer chains. **PEG** was deposited on a gold surface, and the force measurements were carried out in either phosphate-buffered saline (PBS) or hexadecane. The solid line shows the best fit to freely jointed chain (FJC) model, in the case of hexadecane, or two-state FJC model, in the case of PBS. Reprinted figure from Oesterhelt et al. [23] (e) Ring opening of benzocyclobutene with AFM force microscopy at a force of about 920 pN. Polymers containing benzocyclobutene units were absorbed on a silica. Measurements were performed in toluene. Adapted with permission from Wang et al. [24] Copyright © 2015 American Chemical Society. (f) Force versus extension response of poly(isoprene) with 88 kDa **PS** side chains in water and on hydrogen-terminated diamond showing steplike desorption response, and spikelike extension and detachment response. Adapted with permission from Kienle et al. [25]. Copyright © 2014 American Chemical Society.

incorporate a functional group at free end of polymer and investigate specific interactions between the group and the AFM tip or the solid. Investigation of chemical reactions at single-chain or bond level using AFM has led to insights into forces and kinetics of various chemical reactions and transitions, including complexation and coordination [31, 32], receptor-donor type interactions [33], hydrogen bonding [34], and covalent bonding [35, 36]. An example of mechanochemistry at single-chain level is shown in **Figure 1(e)**. AFM force microscopy reveals that the force of opening benzocyclobutene ring is about 1400 pN in toluene, but reduces to 920 pN with the help of an alkene lever arm in the structure of the polymer [24].

Below, I have illustrated AFM application in polymer studies with specific examples. Schematics of the AFM applications in imaging, force microscopy, and other modes are shown in **Figure 2**. The structures of some of the polymers used in the experiments are summarized in **Figure 3**. The polymers are poly(2-vinyl pyridine) (**P2VP**), poly(styrene) (**PS**), poly(ethylene) (**PE**), poly(ethylene glycol) (**PEG**), and a triblock copolymer of poly(exo-N-(2-aminoethyl)-5-norbornene-2,3-dicarboximide) and poly(exo-N-hexyl-5-norbornene-2,3-dicarboximide) (**P1**).

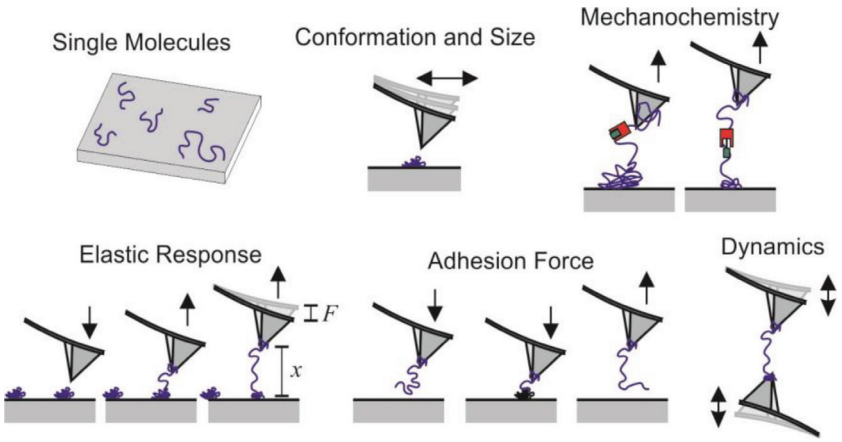

Figure 2. Schematics of AFM imaging of isolated polymer chains, mechanochemistry with AFM, AFM force microscopy of single polymer chains to obtain their elasticity or adhesion forces, and schematic of correlation force spectroscopy (CFS is a variant of AFM) to obtain dynamical mechanical properties of single polymer chains.

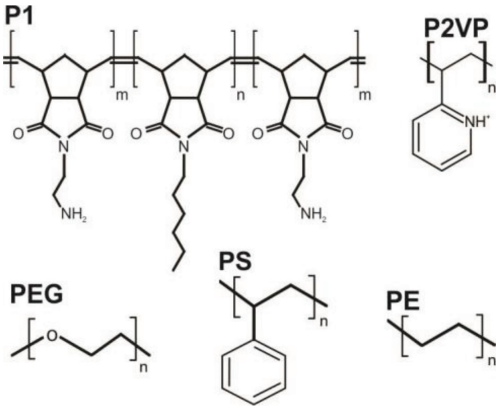

Figure 3. Chemical structure of a triblock copolymer of poly(exo-N-(2-aminoethyl)-5-norbornene-2,3-dicarboximide) and poly(exo-N-hexyl-5-norbornene-2,3-dicarboximide) (**P1**) [37], poly(2-vinyl pyridine) (**P2VP**), poly(ethylene glycol) (**PEG**), poly(styrene) (**PS**), and poly(ethylene) (**PE**). The side blocks of **P1** are about 11 monomers long ($m \approx 11$) and the middle block 544 monomers long ($n \approx 544$). The side blocks contain amine, which enhances bonding of the polymer ends to epoxy-functionalized AFM tip and solid. The covalent bonding helps pull the polymer to high forces of about 1 nN. **P2VP** is positively charged at pH 3.0.

2. Molecular conformations obtained from AFM imaging

Conformation of a single polymer chain may be interpreted in terms of average of spatial correlations between unit vectors **n** tangent to the chain. In the framework of wormlike chain (WLC) model, the average function is of the form:

$$\langle \mathbf{n}(0) \cdot \mathbf{n}(s) \rangle = \exp\left(-\frac{s}{2\ell_p}\right), \tag{1}$$

where s is the length, and ℓ_p is the characteristic decay length of the correlations, or the persistence length. Image analysis software has been developed that tracks the imaged chains and quantify their persistence lengths using Eq. (1) [38].

The correlations generally decay rapidly for thin and flexible polymers, but persist longer for thick and semiflexible polymers, such as double-stranded DNA, which have inherent bending rigidity [3, 18]. For charged polymers such as polyelectrolytes, the persistence length has a contribution from intramolecular electrostatic repulsion, which tends to expand the chain. This contribution may be controlled by pH and the ionic strength of an electrolyte solution. Odijk, Skolnik and Fixman (OSF) theory predicts that the electrostatic contribution decays rapidly with inverse of the ionic strength [39, 40]. However, experiments and simulations generally find a slower decay [18, 41, 42].

Figure 4 shows two AFM images of poly(2-vinyl pyridine) (**P2VP**) polymer chains. The dilute polymer films were prepared as follows. A solution at pH 3.0 was initially prepared by addition of HCl to deionized water. The ionic strength of this solution is approximately 1 mM. To this solution, appropriate amount of NaCl was added to set the ionic strength to 100 mM.

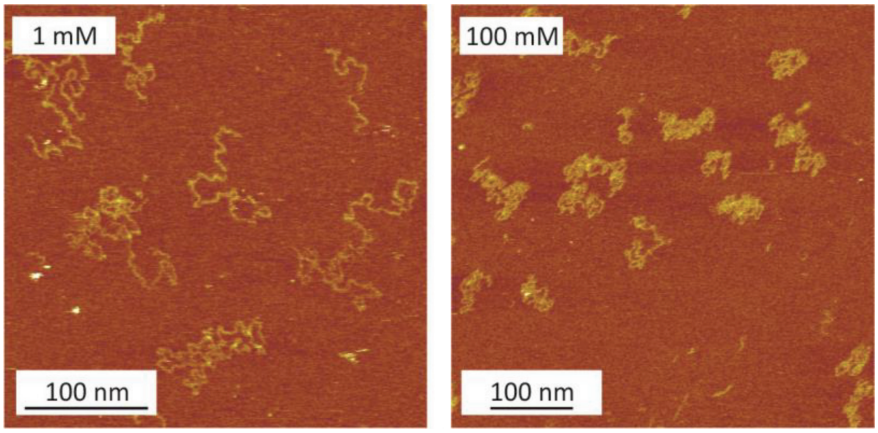

Figure 4. AFM images of poly(2-vinyl pyridine) (**P2VP**) adsorbed on mica at different ionic strength 1 and 100 mM and at pH 3.0. At this pH, **P2VP** is positively charged. At low ionic strength, the molecules form extended random coils due to intramolecular electrostatic repulsion. At high ionic strength, the electrostatic repulsion is screened, and the molecules form partially collapsed coils.

Two **P2VP** solutions were prepared by dissolving the polymer in 1 and 100 mM solutions to a concentration equal to 0.1 mg/L. At pH 3.0, **P2VP** is positively charged due to protonation of nitrogen in pyridine rings. To form a dilute **P2VP** polymer film on mica, 20 mL from 1 or 100 mM polymer solutions were adsorbed on freshly cleaved mica for 40 s. The polymer solution was then replaced with larger volume of the polymer-free electrolyte solution. The adsorbed polymer chains were imaged in amplitude-modulation intermittent contact mode. Silicon tips with nominal tip radius < 10 nm, spring constant in the range of 0.07–0.15 N/m, were used for this purpose. A scan rate of 4.88 Hz with free oscillation amplitude (FOA) of about 10 nm and an amplitude set-point of about 76% of FOA were used. The imaging was carried out at a temperature of 25°C. The image at 1 mM solution shows that the polymer chains form extended random coils on mica. This conformation is due to intramolecular electrostatic repulsion between positively charged monomers. At 100 mM, however, the polymer chains are partially collapsed. The collapse is due to screening of the intramolecular electrostatic repulsion. This observation suggests that, at the lower ionic strength, the electrostatic repulsion contributes largely to the overall conformational persistence of **P2VP** chains. Similar trends have been observed as a function of pH [2].

3. AFM force microscopy of single polymer chains

3.1. Molecular elasticity

From an analysis of the force versus extension response of single polymer chains, one may interpret their elasticity. The elasticity has two contributions: one from the loss of entropy and the other from the deformation of bond angles [23]. Bond angle deformation results in polymer length increasing beyond its contour length (the unperturbed length of polymer chain). The polymer length increases by about 10% at a force of about 2 nN [43].

The crucial step in interpretation of the elasticity of single polymer chains is the identification of single-chain responses, namely that two or more chains are not simultaneously measured. Oversight of this step would result in force responses that are stiffer than the response of an individual chain. It is equally important to ensure that the ends of the polymer chain are strongly adhered to the solid and the AFM tip; that is, the polymer does not slide over the tip or the solid. Sliding would result in softer response than the pure elastic response of the chain.

The force versus extension response is generally interpreted in terms of freely jointed chain (FJC) model [44]:

$$x = L\left[\coth\left(\frac{\ell_K F}{kT}\right) - \frac{kT}{\ell_K F} + \frac{F}{K}\right], \tag{2}$$

where L is the contour length, k is the Boltzmann constant, and T is the absolute temperature. The Kuhn length ℓ_K and the elasticity constant K represent the mechanical properties of single chains. The FJC model has been successful in the analysis of extension responses of flexible polymers, such as synthetic polymers [44].

Figure 5 shows the force versus extension responses of poly(ethylene) (**PE**), which were collected in methyl benzoate and on silica [43]. Polymer solution with concentration 100 mg/L dissolved in toluene was used for deposition. After a deposition period of about 40 s, the polymer-coated silica was rinsed multiple times with toluene to remove loosely bound polymer chains. Thereafter, repeated extension-retraction cycles of the AFM tip to and from polymer coated substrate results in the force-extension responses of single polymer chains. After modeling the individual force responses with the FJC, the extension length of each response was normalized to the fitted contour length. The figure displaying the force versus relative extension profiles shows that the responses from different chains agree reasonably well. The overlap of the profiles asserts that the responses were obtained from single chains. An average Kuhn length $\ell_K = 0.6 \pm 0.1$ nm and an elasticity constant $K = 24 \pm 3$ nN were obtained for **PE**.

Figure 6 shows the force versus relative extension responses of **P2VP** and **PS**. **P2VP** responses were collected in 1 mM, pH 3.0 solution and on mica. Sample preparation was like that explained for AFM images in **Figure 4**. Nanohandling technique was employed to ensure the placement of AFM tip on one end of the adsorbed polymers [5]. An average Kuhn length $\ell_K = 0.5 \pm 0.1$ nm and elasticity constant $K = 9.5 \pm 0.2$ nN were obtained for **P2VP**. Sample preparation in AFM measurements with **PS** was like that explained for **PE**. Measurements in solvents of different quality for **PS** show that the Kuhn length increases with solvent quality. For example, the Kuhn length increases from a value of about 0.27 nm in ethanol to a value of about 0.43 nm in toluene. This finding is akin to swelling of **PS** chains in the respective solvents. Results show an elasticity constant equal to about 21 nN, which remains the same in all solvents.

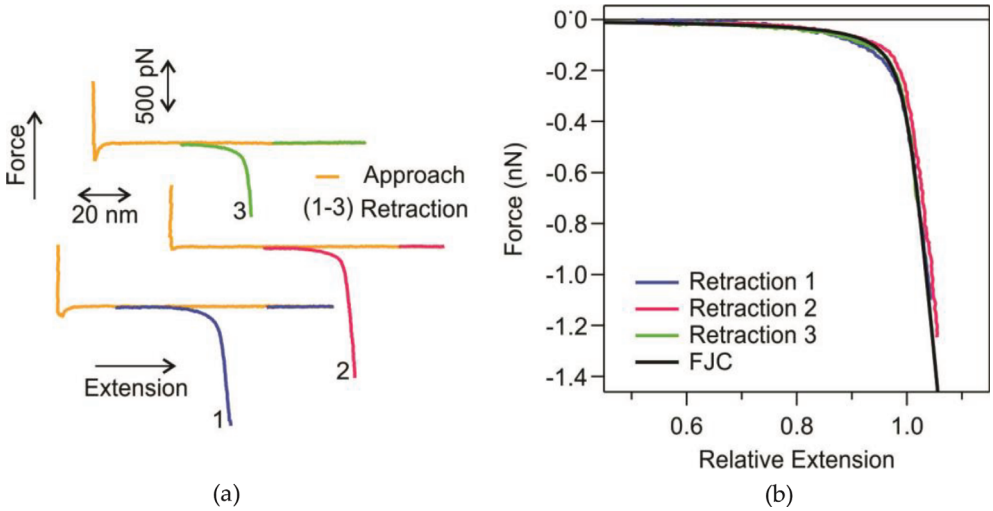

Figure 5. (a) Force versus extension responses of poly(ethylene) (**PE**) obtained from single molecule force microscopy with AFM. Measurements were performed in methyl benzoate and on silica. (b) Force versus relative extension profiles of the same retraction curves shown in (a) together with the freely jointed chain (FJC) curve. The overlap of the profiles shows that the retraction curves are responses of single chains.

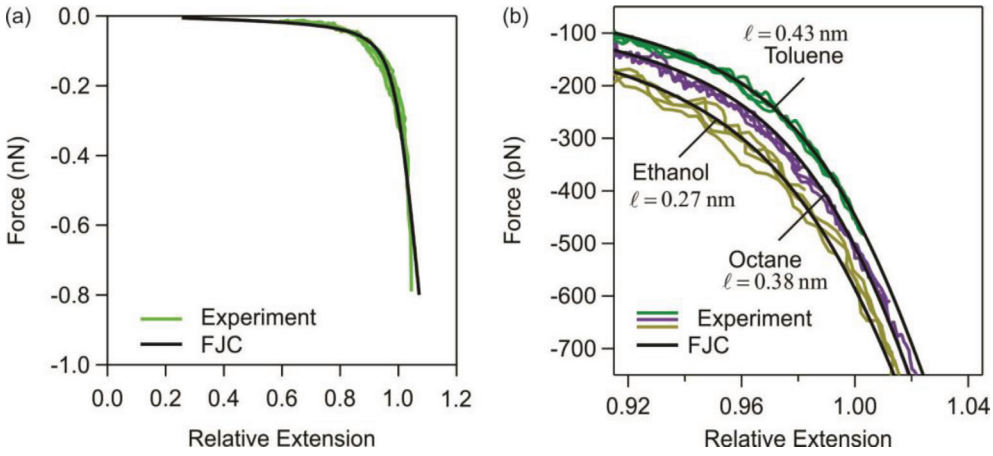

Figure 6. Force versus relative extension responses of (a) poly(2-vinyl pyridine) (**P2VP**) and (b) poly(styrene) **PS** obtained from single molecule force microscopy with AFM together with the freely jointed chain (FJC) curve. Experiments with **P2VP** were performed in pH 3.0 solution, and with **PS** in good solvents, such as toluene, to poor solvents, such as ethanol.

3.2. Adhesion force of single polymer chains

To obtain adhesion interaction forces between single polymer chains and solids, the polymer chains are generally covalently bound to the AFM tip [6, 25, 45]. The polymer chains are brought in contact with the solid. During contact, a single polymer chain may adsorb onto the solid. Upon retraction of the tip, the polymer chain desorbs resulting in a steplike (constant) force response. This force response is then fitted to a sigmoidal model giving the desorption force and length of the polymer-solid interaction.

An example of these studies is shown in **Figure 1(f)** [25]. The force versus extension response of poly(isoprene) with 88 kDa **PS** side chains in water and on hydrogen-terminated diamond shows two force response behaviors. In one case, polymer chains desorb from solid, resulting in steplike response. If two or more polymer chains desorb simultaneously, additional steps are observed in the response. Thereby, the last step is due to the final desorbed polymer chain. The second response behavior involves polymers being extended before detachment from the solid. The desorption force of polymer chains from solid may generally be tuned by the chemical environment of the polymer, polymer chemistry, and the adsorption time on the solid [6, 25].

3.3. Dynamical mechanical properties of single polymer chains

Elasticity of single polymer chains is only one property that defines their response to force. The other property is the relaxation time, or the time it takes for the polymer chain to respond to the force. Lessons from nature, e.g., wing flapping of hummingbirds, tongue projection of salamanders, or eye retraction of slugs, show that these responses are not infinitely fast but take time. This is especially important for end-tethered polymers [46].

Experiments that measure the elasticity and the relaxation time of single polymer chains generally use the thermal fluctuations of an AFM cantilever [47, 48], or externally drive the cantilever by magnetic or acoustic forces [49]. Recently, a correlation force spectroscopy (CFS) is developed that employs two AFM cantilevers in antiparallel configuration as shown in **Figure 7(a)**. The advantage of using two cantilevers in CFS, as compared with one cantilever in AFM, is that in AFM, the proximity of the cantilever to the solid increases the hydrodynamic friction due to thin film lubrication. The increase in the hydrodynamic force (or the hydrodynamic friction coefficient) increases the Brownian forces—a result of fluctuation-dissipation

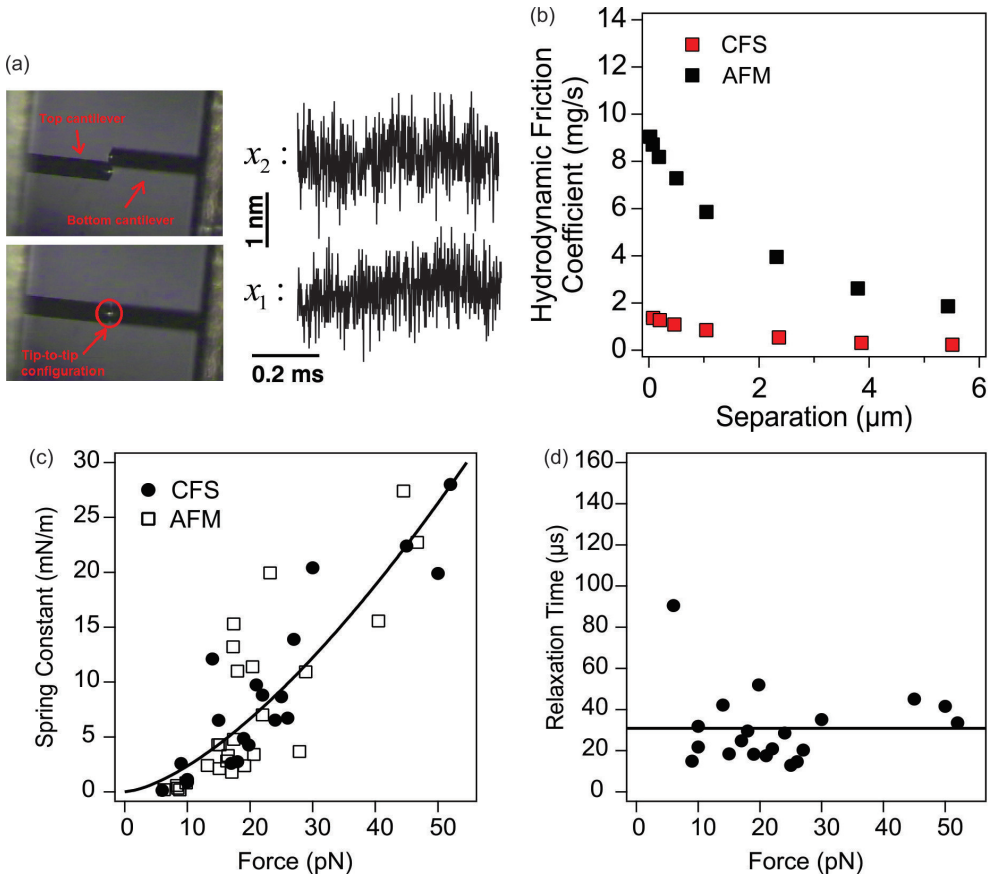

Figure 7. (a) Two AFM cantilevers in antiparallel configuration in a correlation force spectroscopy (CFS) apparatus. In the measurements, thermal fluctuations of the top and bottom cantilevers are collected simultaneously and correlated. (b) Correlation of two cantilevers' fluctuations results in a lower hydrodynamic friction in CFS than the hydrodynamic friction on a single cantilever in AFM. (c) Spring contact of single-stranded DNA measured by CFS and AFM in the force range from about 5 to 50 pN. Solid line is a fit of wormlike chain model (model may be found in Ref. [47]), resulting in persistence length equal to about 2.6 nm. (d) Relaxation time of single-stranded DNA measured by CFS in the force range from about 5 to 50 pN. Solid line is a linear fit (model in Ref. [50]), resulting in a constant value of about 31 μs for the relaxation time.

theorem [51]. Brownian forces result in thermal noise that is the major source of noise in AFM force spectroscopy measurements. Because of the thermal noise and the high hydrodynamic force, AFM force resolution is reduced, and polymer chains may only be examined accurately when extended to high forces. To reduce the high force limit, in AFM applications discussed in the above sections 3.1 and 3.2, one applies a low-pass filter to cantilever deflection signal and thereby discards the time-related or dynamical data. Placement of two AFM cantilevers in the configuration shown in **Figure 7(a)** reduces the hydrodynamic friction and the Brownian forces. **Figure 7(b)** shows a comparison between the hydrodynamic friction coefficient between AFM and CFS. In all separations (in AFM, tip-solid separation, in CFS, tip-tip separation), CFS has a lower hydrodynamic friction coefficient. Similarly, the Brownian forces or the thermal noise are lower in CFS than in AFM. Thereby, CFS has a higher force resolution. CFS also gives the dynamical mechanical properties of single molecules where no filtering is applied in the data analysis [7, 51].

In the measurements, a single polymer chain is tethered between two tips, then extended to a force and clamped. During the clamp period, thermal fluctuations of the top and bottom cantilevers are collected simultaneously. Dynamical mechanical properties of single polymer chains are obtained from an analysis of the time correlations between the two thermal fluctuations. **Figure 7(c)** and **(d)** show the stiffness and the relaxation time of end-tethered single-stranded DNA in the force range from 5 to 50 pN, respectively, [28]. One observes that the stiffness of the chain increases with the force, while the relaxation time remains almost constant equal to about 30 μs. Constant relaxation time is consistent with theory [50].

4. Mechanochemistry at the level of single polymer chains

The force versus extension response of biopolymers, such as double-stranded DNA and various proteins, supramolecules, and polymers containing force-sensitive units, namely mechanophores, generally shows a different behavior. In these polymers, specific structural changes or chemical reactions occur, which are triggered by the application of mechanical force [31–34, 52–55]. The process involves force reducing the energy barrier of transition by an amount $F\Delta x$, where Δx is a length scale associated with the transition length [56]. The reduction in the energy barrier facilitates the transition. For example, the rate of transition increases by a factor $\exp(F\Delta x)$. It has been shown that reactions that do not occur thermally may be triggered by the application of mechanical force [24, 57].

Mechanically induced isomerization of *cis* carbon-carbon double bonds to *trans* conformation in polymer **P1** is shown in **Figure 8** [37]. Experiments were realized by adsorbing polymer chains from a solution with concentration 100 mg/L dissolved in dimethyl sulfoxide (DMSO). The deposition period was 2 hr, after which the solid was rinsed multiple times with DMSO to remove loosely bound chains. Finally, DMSO was added to the solid before the measurements. **Figure 8** shows the force versus extension responses of polymer **P1**, which differ from the force behaviors of **PE**, **P2VP**, and **PS** in **Figures 5** and **6**. In the latter, the force increases with extension until the chain breaks from either the AFM tip or the solid. As shown in **Figure 8**, a

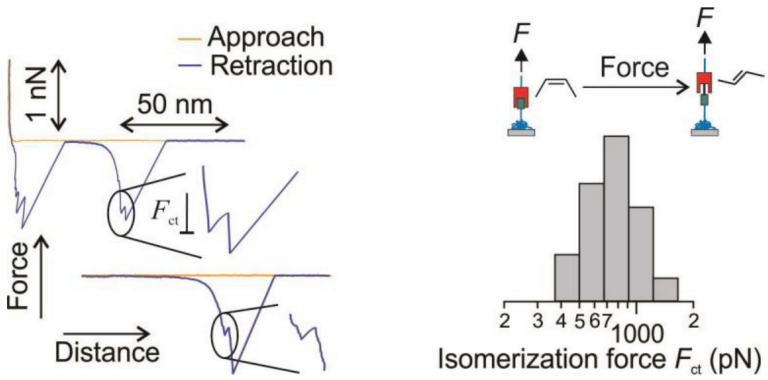

Figure 8. Force versus extension responses of polymer **P1** showing isomerization event. The onset of *cis*-to-*trans* isomerization is shown by a sudden kink in the response profile and is denoted by the isomerization force F_{ct}. The isomerization force has an average value of about 800 pN.

single chain of polymer **P1** is tethered between the AFM tip and the solid even after the isomerization. The force response of **P1** contains a sudden increase in the extension that is due to the isomerization of some *cis* monomers in the backbone of **P1** to *trans* conformation. When isomerization occurs, the force shows a sudden reduction that is due to relaxation of stress on the chain because of extension increase. The force where the isomerization occurs is denoted by F_{ct} and has an average value of about 800 pN. The isomerization force is lower than the force of breaking of covalent bonds and rings, 1–2 nN [57, 58].

5. Conclusions

AFM started as a power imaging technique and soon found its way in the diverse field of polymer studies. In this chapter, the focus was placed on those studies that are at the level of single polymer chains, that is nanoscale. AFM imaging in noncontact mode or intermittent contact mode may be used to obtain conformations and sizes of individual polymer chains. The chains ought to be adsorbed from dilute polymer solutions and on atomically flat solids. AFM force microscopy may be used to obtain the elasticity of single polymer chains. The molecular elasticity in this case is interpreted in terms of an entropic elasticity, which can be tuned by the solvent, and an elasticity term that is due to deformation of bond angles. In the case of force-sensitive polymers, AFM may be used to apply force, and thus trigger specific chemical reactions or conformational transitions in the polymer at the level of single chains and even single bonds. Technical development in AFM has resulted in techniques such as correlation force spectroscopy, which is employed to obtain the dynamical mechanical properties of single polymer chains. Finally, one should note that AFM has also been used to characterize the mechanical properties, such as adhesion, friction, and compression support, of dense polymer films and polymer brushes. This level of investigation is not single-molecule level and thereby was not included in this chapter.

Acknowledgements

Research performed by M.R. has received funding from the National Science Foundation of the United States via Award Number CBET-0959228, the National Center of Competence in Research for Bio-Inspired Materials in Switzerland, Virginia Tech, and University of Geneva. These researches were performed in the laboratory of Prof. William Ducker and in the laboratory of Prof. Michal Borkovec. M.R. acknowledges collaborations, useful discussions, and contributions from Prof. Mark Paul, Prof. John Walz, Prof. Andreas Kilbinger, Dr. Christopher Honig, Dr. Plinio Maroni, Dr. Brian Robbins, Dr. Lucie Grebikova, Svilen Kozhuharov, and Phally Kong.

Author details

Milad Radiom

Address all correspondence to: miradi@kth.se

KTH Royal Institute of Technology, Stockholm, Sweden

References

[1] Binnig G, Quate CF, Gerber C. Atomic force microscope. Physical Review Letters. 1986; **56**(9):930-933

[2] Roiter Y, Minko S. AFM single molecule experiments at the solid−liquid Interface: In situ conformation of adsorbed flexible polyelectrolyte chains. Journal of the American Chemical Society. 2005;**127**(45):15688-15689

[3] Japaridze A, Vobornik D, Lipiec E, Cerreta A, Szczerbinski J, Zenobi R, et al. Toward an effective control of DNA's submolecular conformation on a surface. Macromolecules. 2016;**49**(2):643-652

[4] Rief M, Gautel M, Oesterhelt F, Fernandez JM, Gaub HE. Reversible unfolding of individual titin immunoglobulin domains by AFM. Science. 1997;**276**(5315):1109-1112

[5] Grebikova L, Radiom M, Maroni P, Schlüter DA, Borkovec M. Recording stretching response of single polymer chains adsorbed on solid substrates. Polymer. 2016;**102**:350-362

[6] Geisler M, Netz RR, Hugel T. Pulling a single polymer molecule off a substrate reveals the binding thermodynamics of cosolutes. Angewandte Chemie International Edition. 2010; **49**(28):4730-4733

[7] Radiom M, Honig CDF, Walz JY, Paul MR, Ducker WA. A correlation force spectrometer for single molecule measurements under tensile load. Journal of Applied Physics. 2013; **113**(1):013503

[8] Netz RR. Strongly stretched semiflexible extensible polyelectrolytes and DNA. Macromolecules. 2001;**34**(21):7522-7529

[9] Dobrynin AV, Carrillo J-MY, Rubinstein M. Chains are more flexible under tension. Macromolecules. 2010;**43**(21):9181-9190

[10] Livadaru L, Netz RR, Kreuzer HJ. Interacting chain model for poly(ethylene glycol) from first principles—Stretching of a single molecule using the transfer matrix approach. Journal of Chemical Physics. 2003;**118**(3):1404-1416

[11] Hugel T, Rief M, Seitz M, Gaub HE, Netz RR. Highly stretched single polymers: Atomic-force-microscope experiments versus ab-initio theory. Physical Review Letters. 2005;**94**(4): 048301

[12] Oliveira Brett AM, Chiorcea Paquim A-M. DNA imaged on a HOPG electrode surface by AFM with controlled potential. Bioelectrochemistry. 2005;**66**(1):117-124

[13] Kiriy A, Gorodyska G, Kiriy N, Sheparovych R, Lupytsky R, Minko S, et al. AFM imaging of single polycation molecules contrasted with cyanide-bridged compounds. Macromolecules. 2005;**38**(2):501-506

[14] Lauritsen JV, Reichling M. Atomic resolution non-contact atomic force microscopy of clean metal oxide surfaces. Journal of Physics: Condensed Matter. 2010;**22**(26):263001

[15] Marchand DJ, Hsiao E, Kim SH. Non-contact AFM imaging in water using electrically driven cantilever vibration. Langmuir. 2013;**29**(22):6762-6769

[16] Grebikova L, Maroni P, Zhang B, Schlüter AD, Borkovec M. Single-molecule force measurements by nano-handling of individual dendronized polymers. ACS Nano. 2014;**8**(3): 2237-2245

[17] Adamcik J, Klinov DV, Witz G, Sekatskii SK, Dietler G. Observation of single-stranded DNA on mica and highly oriented pyrolytic graphite by atomic force microscopy. FEBS Letters. 2006;**580**(24):5671-5675

[18] Grebikova L, Kozhuharov S, Maroni P, Mikhaylov A, Dietler G, Schluter AD, et al. The persistence length of adsorbed dendronized polymers. Nanoscale. 2016;**8**(27):13498-13506

[19] Roiter Y, Trotsenko O, Tokarev V, Minko S. Single molecule experiments visualizing adsorbed polyelectrolyte molecules in the full range of mono- and divalent counterion concentrations. Journal of the American Chemical Society. 2010;**132**(39):13660-13662

[20] Kiriy A, Gorodyska G, Minko S, Jaeger W, Stepanek P, Stamm M. Cascade of coil-globule conformational transitions of single flexible polyelectrolyte molecules in poor solvent. Journal of the American Chemical Society. 2002;**124**(45):13454-13462

[21] Roiter Y, Jaeger W, Minko S. Conformation of single polyelectrolyte chains vs. salt concentration: Effects of sample history and solid substrate. Polymer. 2006;**47**(7):2493-2498

[22] Zhang B, Wepf R, Kröger M, Halperin A, Schlüter AD. Height and width of adsorbed dendronized polymers: Electron and atomic force microscopy of homologous series. Macromolecules. 2011;**44**(17):6785-6792

[23] Oesterhelt F, Rief M, Gaub HE. Single molecule force spectroscopy by AFM indicates helical structure of poly(ethylene-glycol) in water. New Journal of Physics. 1999;**1**:6.1-6.11

[24] Wang J, Kouznetsova TB, Niu Z, Rheingold AL, Craig SL. Accelerating a mechanically driven anti-Woodward–Hoffmann ring opening with a polymer lever arm effect. The Journal of Organic Chemistry. 2015;**80**(23):11895-11898

[25] Kienle S, Gallei M, Yu H, Zhang B, Krysiak S, Balzer BN, et al. Effect of molecular architecture on single polymer adhesion. Langmuir. 2014;**30**(15):4351-4357

[26] Livadaru L, Netz RR, Kreuzer HJ. Stretching response of discrete semiflexible polymers. Macromolecules. 2003;**36**(10):3732-3744

[27] Shi WQ, Giannotti MI, Zhang X, Hempenius MA, Sconherr H, Vancso GJ. Closed mechanoelectrochemical cycles of individual single-chain macromolecular motors by AFM. Angewandte Chemie International Edition. 2007;**46**(44):8400-8404

[28] Radiom M, Paul MR, Ducker WA. Dynamics of single-stranded DNA tethered to a solid. Nanotechnology. 2016;**27**(25):255701

[29] Balzer BN, Kienle S, Gallei M, von Klitzing R, Rehahn M, Hugel T. Stick-slip mechanisms at the nanoscale. Soft Materials. 2014;**12**(sup1):S106-S114

[30] Balzer BN, Gallei M, Hauf MV, Stallhofer M, Wiegleb L, Holleitner A, et al. Nanoscale friction mechanisms at solid-liquid interfaces. Angewandte Chemie International Edition. 2013;**52**(25):6541-6544

[31] Auletta T, de Jong MR, Mulder A, van Veggel F, Huskens J, Reinhoudt DN, et al. Beta-cyclodextrin host-guest complexes probed under thermodynamic equilibrium: Thermodynamics and AFM force spectroscopy. Journal of the American Chemical Society. 2004; **126**(5):1577-1584

[32] Kado S, Kimura K. Single complexation force of 18-crown-6 with ammonium ion evaluated by atomic force microscopy. Journal of the American Chemical Society. 2003;**125**(15):4560-4564

[33] Skulason H, Frisbie CD. Direct detection by atomic force microscopy of single bond forces associated with the rupture of discrete charge-transfer complexes. Journal of the American Chemical Society. 2002;**124**(50):15125-15133

[34] Embrechts A, Velders AH, Schonherr H, Vancso GJ. Self-complementary recognition of supramolecular urea-aminotriazines in solution and on surfaces. Langmuir. 2011;**27**(23): 14272-14278

[35] Schuetze D, Holz K, Mueller J, Beyer MK, Luening U, Hartke B. Pinpointing mechanochemical bond rupture by embedding the mechanophore into a macrocycle. Angewandte Chemie, International Edition. 2015;**54**(8):2556-2559

[36] Klukovich HM, Kouznetsova TB, Kean ZS, Lenhardt JM, Craig SL. A backbone lever-arm effect enhances polymer mechanochemistry. Nature Chemistry. 2013;**5**(2):110-114

[37] Radiom M, Kong P, Maroni P, Schafer M, Kilbinger AFM, Borkovec M. Mechanically induced cis-to-trans isomerization of carbon-carbon double bonds using atomic force microscopy. Physical Chemistry Chemical Physics. 2016;**18**(45):31202-31210

[38] Mikhaylov A, Sekatskii S, Dietler G. DNA trace: A comprehensive software for polymer image processing. Journal of Advanced Microscopy Research. 2013;**8**(4):241-245

[39] Odijk T. Polyelectrolytes near the rod limit. Journal of Polymer Science. 1977;**15**(3):477-483

[40] Skolnick J, Fixman M. Electrostatic persistence length of a wormlike polyelectrolyte. Macromolecules. 1977;**10**(5):944-948

[41] Netz RR, Orland H. Variational theory for a single polyelectrolyte chain. European Physical Journal B. 1999;**8**(1):81-98

[42] Ullner M. Comments on the scaling behavior of flexible polyelectrolytes within the Debye−Hückel approximation. The Journal of Physical Chemistry B. 2003;**107**(32):8097-8110

[43] Radiom M, Maroni P, Wesolowski TA. Size extensivity of elastic properties of alkane fragments. Journal of Molecular Modeling. 2018;**24**:36

[44] Giannotti MI, Vancso GJ. Interrogation of single synthetic polymer chains and polysaccharides by AFM-based force spectroscopy. Chemphyschem. 2007;**8**(16):2290-2307

[45] Grebikova L, Gojzewski H, Kieviet BD, Gunnewiek MK, Vancso GJ. Pulling angle-dependent force microscopy. The Review of Scientific Instruments. 2017;**88**(3):033705

[46] Berkovich R, Hermans RI, Popa I, Stirnemann G, Garcia-Manyes S, Berne BJ, et al. Rate limit of protein elastic response is tether dependent. Proceedings of the National Academy of Sciences. 2012;**109**(36):14416-14421

[47] Khatri BS, Byrne K, Kawakami M, Brockwell DJ, Smith DA, Radford SE, et al. Internal friction of single polypeptide chains at high stretch. Faraday Discussions. 2008;**139**(0):35-51

[48] Kawakami M, Byrne K, Khatri B, McLeish TCB, Radford SE, Smith DA. Viscoelastic properties of single polysaccharide molecules determined by analysis of thermally driven oscillations of an atomic force microscope cantilever. Langmuir. 2004;**20**(21):9299-9303

[49] Kawakami M, Byrne K, Khatri BS, McLeish TCB, Radford SE, Smith DA. Viscoelastic measurements of single molecules on a millisecond time scale by magnetically driven oscillation of an atomic force microscope cantilever. Langmuir. 2005;**21**(10):4765-4772

[50] Hiraiwa T, Ohta T. Linear viscoelasticity of a single semiflexible polymer with internal friction. The Journal of Chemical Physics. 2010;**133**(4):044907

[51] Honig CDF, Radiom M, Robbins BA, Walz JY, Paul MR, Ducker WA. Correlations between the thermal vibrations of two cantilevers: Validation of deterministic analysis via the fluctuation-dissipation theorem. Applied Physics Letters. 2012;**100**(5):053121

[52] Liese S, Gensler M, Krysiak S, Schwarzl R, Achazi A, Paulus B, et al. Hydration effects turn a highly stretched polymer from an entropic into an energetic spring. ACS Nano. 2017; **11**(1):702-712

[53] Marszalek PE, Li H, Oberhauser AF, Fernandez JM. Chair-boat transitions in single polysaccharide molecules observed with force-ramp AFM. Proceedings of the National Academy of Sciences of the United States of America. 2002;**99**(7):4278-4283

[54] Clausen-Schaumann H, Rief M, Tolksdorf C, Gaub HE. Mechanical stability of single DNA molecules. Biophysical Journal. 2000;**78**(4):1997-2007

[55] Hosono N, Kushner AM, Chung J, Palmans ARA, Guan Z, Meijer EW. Forced unfolding of single-chain polymeric nanoparticles. Journal of the American Chemical Society. 2015; **137**(21):6880-6888

[56] Bell GI. Models for specific adhesion of cells to cells. Science. 1978;**200**(4342):618-627

[57] Wang J, Kouznetsova TB, Niu Z, Ong MT, Klukovich H, Rheingold AL, et al. Inducing and quantifying forbidden reactivity with single-molecule polymer mechanochemistry. Nature Chemistry. 2015;**7**(4):323-327

[58] Grandbois M, Beyer M, Rief M, Clausen-Schaumann H, Gaub HE. How strong is a covalent bond? Science. 1999;**283**(5408):1727-1730